Type-II phase-matched second-harmonic generation in ferroelectric liquid crystals

J. Etxebarria, Naia Pereda, and C. L. Folcia
Departamento de Física de la Materia Condensada, Facultad de Ciencias, Universidad del País Vasco, Apartado Postal 644, 48080 Bilbao, Spain

J. Ortega
Departamento de Física Aplicada II, Facultad de Ciencias, Universidad del País Vasco, Apartado Postal 644, 48080 Bilbao, Spain
(Received 14 October 1997)

The experimental configurations that permit phase-matched second-harmonic generation in ferroelectric liquid crystals have been analyzed. The materials have been assumed to behave as uniaxial positive with normal wavelength dispersion of refractive indices. It has been found that both type I and type II phase matching are possible for a general configuration and the corresponding effective second-order susceptibility coefficients have been calculated. However, with the usual homeotropic geometry, only type I phase matching can be achieved. Under planar alignment, types I and II are accessible in theory, but the large birefringence of most materials usually prevents both possibilities. Nevertheless, a compound, whose properties are suitable for type II phase matching observation, has been found. The effect has been confirmed experimentally and the results agree well with the theory. [S1063-651X(98)08705-4]

PACS number(s): 42.70.Df, 42.65.Ky

I. INTRODUCTION

Second-harmonic generation (SHG) in ferroelectric liquid crystals (FLC's) has recently received much attention in connection with the potential use of these materials in photonics [1–4]. As is well known, the SHG process is most efficient when the so-called phase-matching (PM) condition is fulfilled [5]. At PM the whole crystal participates in the second-harmonic conversion, whereas if there is a phase mismatch Δk, the crystal length that is useful in producing the second-harmonic power is restricted to the so-called coherence length $\ell_c = \pi/\Delta k$.

If two waves of frequency ω and polarizations j and k combine to give a wave of frequency 2ω and polarization i, then the phase mismatch is given by $\Delta k = k_{2\omega}^{(i)} - k_{\omega}^{(j)} - k_{\omega}^{(k)}$. Here we have assumed that i, j, and k describe linear polarized waves whose polarization directions coincide with those of the eigenmodes of propagation in the crystal. $k_{2\omega}$ and k_{ω} refer to the wave vectors for the second-harmonic and fundamental beams, respectively. Two different types of PM are commonly distinguished in the literature [5]. In type I $j = k$, while in type II $j \neq k$.

It is a well known fact that SHG in FLC's is phase matchable. This characteristic was already found in the early experiments [6,7] and is due to the large birefringence of the materials and their relative low dispersion. Assuming the uniaxial approximation, the process is described as $ee \rightarrow o$ (two extraordinary waves at ω produce a 2ω ordinary wave) and, therefore, the PM is classified as type I. The experiment is typically performed on a homeotropic geometry, in which the angle of incidence for PM is easily accessible (typically 0°–30°). Evidently, given the low symmetry of FLC's (point group C_2), it is to be expected that some other experimental configurations can give rise to PM as well. The purpose of this paper is to analyze this problem in detail. We will find that several possibilities for both types of PM do indeed exist, but, unfortunately, are not easily observable in practice using the common alignments (homeotropic or planar) in liquid crystals. However, we will present measurements of one material in which type II phase-matched SHG is successfully demonstrated.

II. THEORY

In this section we will examine the configurations for phase-matched SHG in FLC's. We will assume that the materials behave as positive uniaxial and show normal dispersion. This does not represent any important restriction for slightly colored (or transparent) compounds.

The experimental geometry is indicated in Fig. 1. The light is incident along the negative direction of the laboratory Z axis, which makes polar and azimuthal angles θ and ϕ with respect to the coordinate system (x,y,z) attached to the material. Here, z is along the molecular director $\mathbf{n}$ and y along the direction of the spontaneous polarization $\mathbf{P}_s$. Finally the X axis of the laboratory frame lies on the Zz plane.

In the laboratory system, the polarization eigenmodes for light propagating along Z have components (1,0,0) and (0,1,0), with refractive indices $n_e(\theta)$ and n_o, where $n_e(\theta)$ is given by

$$\left(\frac{1}{n_e(\theta)}\right)^2 = \frac{\sin^2\theta}{n_e^2} + \frac{\cos^2\theta}{n_o^2}, \tag{1}$$

where n_o and n_e are the ordinary and extraordinary indices of the material.

The electric field amplitude of the second-harmonic generated by incoming light with frequency ω and electric field components E_j^{ω} $(j = X,Y)$ can be expressed as [8]

$$E_i^{2\omega} = \sum_{j,k} \omega \left(\frac{\mu_0}{\varepsilon}\right)^{1/2} d_{ijk} E_j^{\omega} E_k^{\omega} \frac{1 - e^{i\Delta k L}}{\Delta k}, \quad i = X,Y, \tag{2}$$

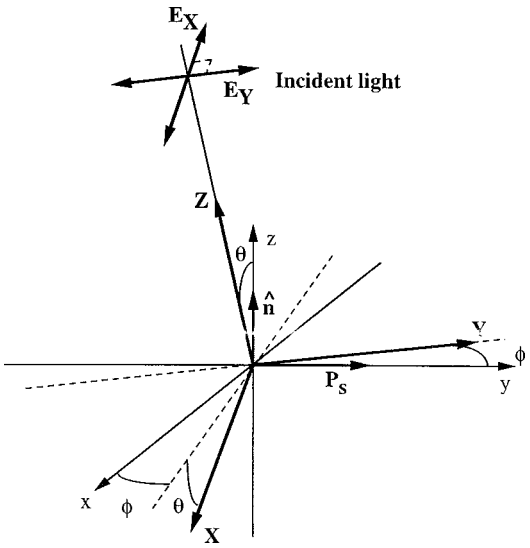

FIG. 1. Schematic view of the laboratory (X,Y,Z) and sample (x,y,z) coordinate systems used to analyze the SHG process in FLC's. The light comes along the negative direction of Z, which makes polar and azimuthal angles θ and ϕ with respect to the sample frame. The polarization eigenmodes of the incoming light are along X (extraordinary) and Y (ordinary). The sample system is taken with the z axis along the molecular director **n** and the y axis along the spontaneous polarization $\mathbf{P}_s$.

where Δk is the phase mismatch defined above, L the interaction length, and d_{ijk} are the coefficients of the second-order susceptibility tensor for SHG referred to the laboratory frame. In Eq. (2), ε represents an average permittivity of the material for optical frequencies and μ_0 is the magnetic permeability of vacuum.

There are in general four terms on the right-hand side of Eq. (2) (although the two cross terms d_{ijk} and d_{ikj} are equal). However, if PM occurs $(\Delta k=0)$, one term is usually dominant over the rest. Under these conditions, the standard formula for the second harmonic power $P^{2\omega}$ is obtained [9]:

$$P^{2\omega}\propto d_{\mathrm{eff}}^2 L^2\ \mathrm{sinc}^2\left(\frac{\Delta kL}{2}\right), \tag{3}$$

where d_{eff} is the so-called effective d coefficient. This parameter coincides with the d_{ijk} element for which the PM takes place (type I) or is equal to $2d_{ijk}$ (type II). In Eq. (3), $\mathrm{sinc}x=\sin x/x$.

Now, in the case of FLC's, there are two possibilities for PM (see Fig. 2). These are denoted as $ee\rightarrow o$ (type I) and $eo\rightarrow o$ (type II). For the first case the relevant coefficient is $d_{\mathrm{eff}}^{\mathrm{I}}=d_{YXX}$ and for the second case we have $d_{\mathrm{eff}}^{\mathrm{II}}=2d_{YYX}$. These coefficients depend on the direction of incidence of the fundamental beam and on the material d tensor. This tensor is usually expressed with reference to the sample coordinate system and, assuming Kleinman conditions, takes the form

$$d=\begin{pmatrix} 0 & 0 & 0 & d_{14} & 0 & d_{21} \\ d_{21} & d_{22} & d_{23} & 0 & d_{14} & 0 \\ 0 & 0 & 0 & d_{23} & 0 & d_{14} \end{pmatrix} \tag{4}$$

in reduced notation. Making the transformation between laboratory and sample axes we finally get

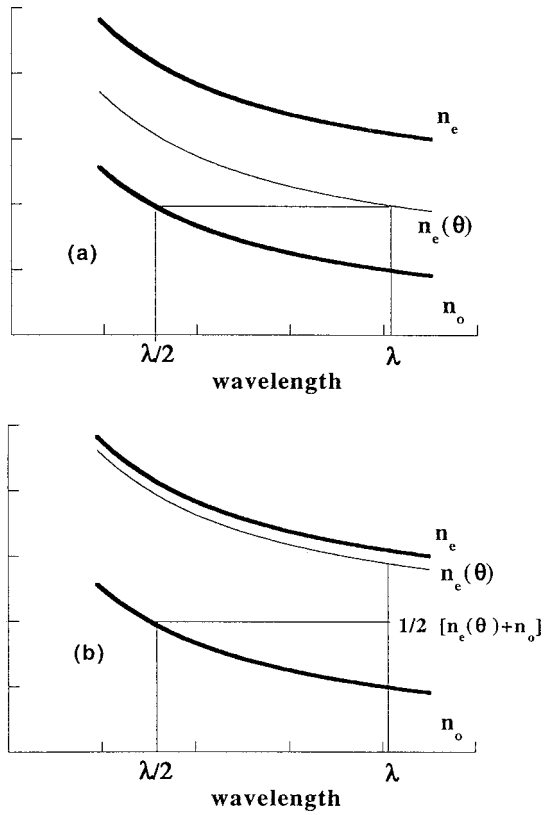

FIG. 2. Wavelength dispersion of the ordinary n_0 and extraordinary n_e refractive indices in FLC's. $n_e(\theta)$ is the extraordinary index when the incident light propagates along a direction that makes an angle θ with the molecular director. The two possibilities for PM are illustrated. Type I PM $(ee\rightarrow o)$ is achieved (a) when the condition $n_0^{2\omega}=n_e^{\omega}(\theta)$ is fulfilled. Type II PM $(eo\rightarrow o)$ is attained (b) when $n_0^{2\omega}=[n_0^{2\omega}+n_e^{\omega}(\theta)]/2$.

$$\begin{aligned} d_{\mathrm{eff}}^{\mathrm{I}}=&-d_{14}\sin 2\theta\cos 2\phi+d_{21}\cos^2\theta\cos\phi(\cos^2\phi \\ &-2\sin^2\phi)+d_{22}\cos^2\theta\cos\phi\sin^2\phi \\ &+d_{23}\sin^2\theta\cos\phi, \end{aligned} \tag{5}$$

$$\begin{aligned} d_{\mathrm{eff}}^{\mathrm{II}}=&-2d_{14}\sin\theta\sin 2\phi+2d_{21}\cos\theta\sin\phi(2\cos^2\phi \\ &-\sin^2\phi)-2d_{22}\cos\theta\sin\phi\cos^2\phi. \end{aligned} \tag{6}$$

These equations together with the condition $\Delta k=0$, that is, $n_o^{2\omega}=n_e^{\omega}(\theta)$ and $n_o^{2\omega}=[n_o^{\omega}+n_e^{\omega}(\theta)]/2$ for types I and II, respectively, define the PM angular positions and SHG efficiencies. These last equations can be simplified somewhat by approximating Eq. (1) to $n_e^{\omega}(\theta)\approx n_o^{\omega}+\Delta n\sin^2\theta$, where $\Delta n=n_e^{\omega}-n_o^{\omega}$ is the birefringence at the fundamental frequency [7]. We get

$$\sin^2\theta=\Delta n_d/\Delta n \tag{7}$$

for type I PM and

$$\sin^2\theta=2\Delta n_d/\Delta n \tag{8}$$

for type II PM, where $\Delta n_d=n_o^{2\omega}-n_o^{\omega}$ accounts for the dispersion of the material.

We now turn to analyze these results in special cases. The PM position can be only achieved by tuning the θ angle in

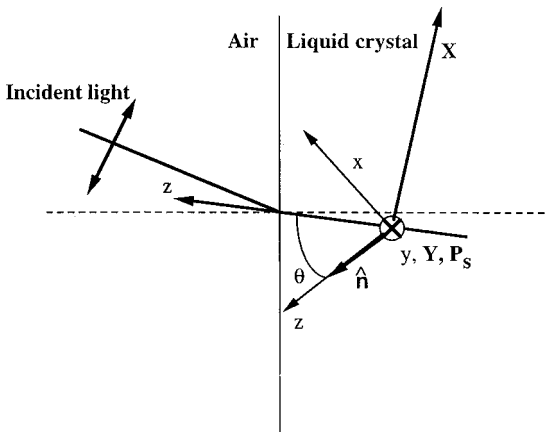

FIG. 3. Experimental geometry for observing phase-matched SHG in homeotropically aligned FLC's. The helix in the Sm-C^* phase is unwound by an electric field parallel to the y axis. The light propagates on the tilt plane. The (type I) PM condition is found by rotating the sample about the y axis. Type II PM is not possible.

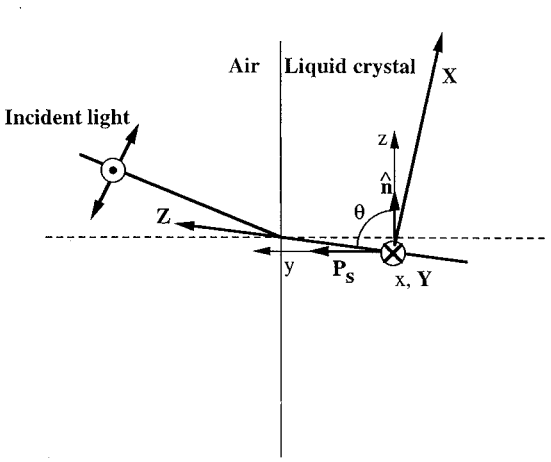

FIG. 4. Experimental geometry for observing phase-matched SHG in planar samples. The helix in the Sm-C^* phase is unwound by an electric field parallel to the y axis. The PM condition is found by rotating the material about the x axis. Both types I and II PM can be reached in principle. However, in most materials the required θ value is so small that Snell's law does not allow this situation to be achieved.

order to vary $n_e^{\omega}(\theta)$. This can be accomplished by rotating the sample about the Y axis with a fixed incident light direction. On the other hand, only the configurations with either $\phi=0$ or $\phi=\pi/2$ are accessible in practice. The first one is available using homeotropic orientation while the second can be achieved typically under planar alignment. We will be restricted to treating these two important cases.

For light propagation on the tilt plane (Fig. 3) we have $\phi=0$. Then $d_{\text{eff}}^{\text{II}}=0$ and $d_{\text{eff}}^{\text{I}}$ takes the more familiar form

$$d_{\text{eff}}^{\text{I}}=-d_{14}\sin 2\theta+d_{21}\cos^2\theta+d_{23}\sin^2\theta. \tag{9}$$

This is the configuration where most experiments have been performed. There is no type II PM, and, to achieve maximum conversion in type I, the fundamental light should be polarized along X.

The second possibility to be discussed occurs for $\phi=\pi/2$. Equations (5) and (6) then reduce to

$$d_{\text{eff}}^{\text{I}}=d_{14}\sin 2\theta, \tag{10}$$

$$d_{\text{eff}}^{\text{II}}=-2d_{21}\cos\theta \tag{11}$$

and, therefore, both types of PM can in principle be observed.

On the other hand, it is interesting to have an estimate of the θ angle required to observe both types of PM. Taking birefringence and dispersion values typical for FLC's $\Delta n=0.2$, $\Delta n_d=0.03$ [10], Eqs. (7) and (8) yield $\theta=23°$ and $\theta=33°$ for types I and II, respectively. The size of θ permits one to detect easily type I PM using homeotropic samples (Fig. 3). Due to the existence of a molecular tilt angle θ_t of nearly the same magnitude as θ, the phenomenon occurs close to normal incidence, as has been determined by many experiments. In contrast, θ values are too small to permit the observation of PM using planar samples, since the angles of refraction are strongly limited by Snell's law (Fig. 4). In particular, this would explain the lack of observations of type II PM up to now. In order to achieve this objective, materials with smaller Δn and/or larger Δn_d are required. We will return to this point in the next section.

III. EXPERIMENTAL RESULTS AND DISCUSSION

The chemical structure of the compound selected for this study is shown in Fig. 5. It belongs to a family of *ortho*-platinated β-diketonate complexes whose nonlinear optical properties have been reported elsewhere [11]. Although the molecule has not the typical rodlike shape, the material behaves optically the same as conventional FLC's [11]. The temperature dependences of θ_t and P_s are classical, with saturation values $\theta_t=30°$ and $P_s=55\ \text{nC/cm}^2$. Likewise, both linear and nonlinear optical properties are compatible with point group C_2 for the ferroelectric phase, which is characteristic of a normal smectic-C^*(Sm-C^*) structure. However, as is explained below, the values of Δn and Δn_d are a bit unusual in comparison with those of calamitic FLC's.

For a frequency ω corresponding to a wavelength $\lambda=1064$ nm (the light of a Nd:YAG laser), the material has a

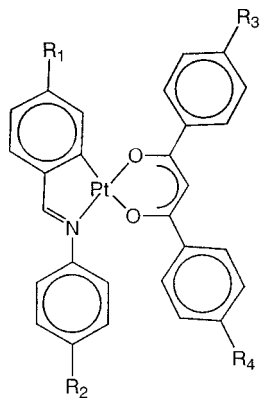

R_1 : O*CH(CH$_3$)C$_6$H$_{13}$ R_2, R_3, R_4 : OC$_{10}$H$_{21}$
I 127°C S_A 112°C S_C* 75°C C

FIG. 5. Chemical structure and phase sequence on cooling of the compound studied.

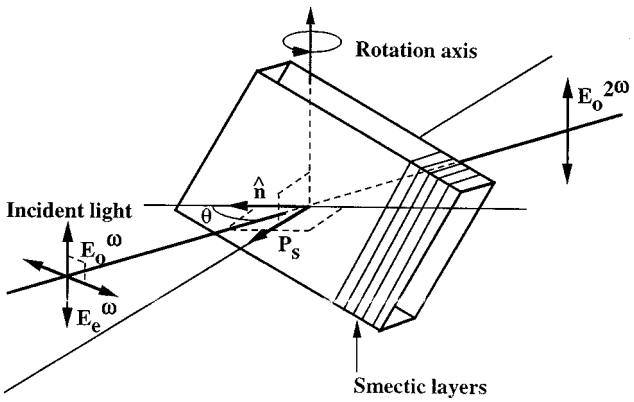

FIG. 6. Experimental geometry for detecting type II phase-matched SHG. The helix is unwound by an electric field perpendicular to the substrate surface. The θ angle was varied by rotating the sample about a vertical axis, which was perpendicular to the molecular director and spontaneous polarization. The fundamental light was polarized at 45° and the second harmonic beam was polarized on the vertical plane.

rather low birefringence in the Sm-C^* phase, with $\Delta n = 0.076$ at the Sm-A–Sm-C^* transition point, increasing to $\Delta n = 0.095$ at 20 °C below the ferroelectric transition [11]. On the other hand, the dispersion of the material is somewhat high (presumably due to the presence of absorption bands at the green-blue part of the spectrum); $\Delta n_d = 0.043$, practically constant all over the Sm-C^* range [11]. With these data and using Eq. (8) we get a θ value for type II PM in the range of 70°. For the geometry of Fig. 4 and assuming an average refractive index of 1.6, this means an angle of incidence of about 35°, which in principle is experimentally achievable.

The experiment was performed using the configuration schematized in Fig. 6. The sample was planarly aligned in a glass cell treated with nylon 6/6, which was deposited using the procedure described in Ref. [12]. Rather good alignment was attained given the large sample thickness (59 μm), although some defects were visible over most of the sample area. Obviously, better alignment quality could have been achieved with thinner cells. However, here it was important to have a sample where the interaction length was as large as possible in order to make evident the PM contribution to the second-harmonic signal. A dc electric field of 2 V/μm perpendicular to the glass plates was applied to the sample to unwind the helix in the Sm-C^* phase. The temperature was kept fixed during the measurements at $T = 90$ °C. At this temperature it was checked with a polarizing microscope that the molecular director had the desired horizontal disposition.

The setup for SHG measurements was described elsewhere [13]. The fundamental light came from a Q-switched Nd:YAG laser. The plane of polarization of the incident light made an angle of 45° with the horizontal plane in order to maximize the type II PM contribution to the second-harmonic signal. The sample was rotated about the vertical axis and the experiment was carried out by monitoring the component of the second-harmonic light polarized in the vertical plane as a function of the angle of incidence.

Under these conditions and according to Eq.(2), the amplitude of the second-harmonic field along the vertical direction is given by

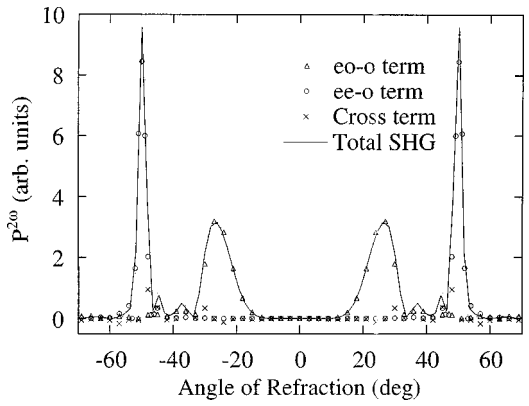

FIG. 7. Calculated values of $P^{2\omega}$ for the experimental disposition of Fig. 6. The optical data were taken from Ref. [11]. The three contributions to the total SHG signal are separated. The peaks corresponding to type I PM (ee-o term) and type II PM (eo-o term) are clearly visible.

$$E_Y^{2\omega} = \omega\left(\frac{\mu_0}{\varepsilon}\right)^{1/2}\left\{ d_{14}\sin 2\theta\,\frac{1-e^{i\Delta k_1 L}}{\Delta k_1} - 2d_{21}\cos\theta\,\frac{1-e^{i\Delta k_2 L}}{\Delta k_2}\right\}\frac{(E^{\omega})^2}{2}, \tag{12}$$

where

$$\Delta k_1 = \frac{4\pi}{\lambda}\left[n_0^{2\omega} - n_e^{\omega}(\theta)\right] \tag{13}$$

and

$$\Delta k_2 = \frac{4\pi}{\lambda}\left\{ n_0^{2\omega} - \frac{1}{2}\left[n_e^{\omega}(\theta) + n_0^{\omega}\right]\right\}. \tag{14}$$

The second-harmonic power $P^{2\omega}$ can be obtained by squaring Eq. (12). Clearly three contributions appear. Two of them are of the form of Eq. (3) and correspond to the terms that give rise to types I and II PM. The third term is the cross term and is negligible if large interaction lengths are used. In Fig. 7 these three terms and the whole SHG have been plotted for our sample as a function of the internal angle of refraction. For this plot, d_{ij}, Δn, and Δn_d were taken from Ref. [11].

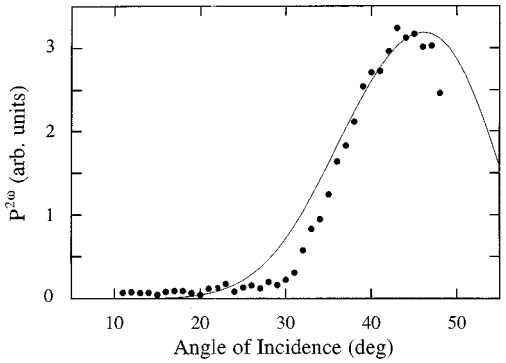

FIG. 8. Experimental SHG signal (dots) as a function of the angle of incidence for the geometry of Fig. 6. The continuous line corresponds to the simulation results.

As can be seen, the second-harmonic intensity profile is symmetric with respect to the normal incidence position. On the other hand, it should be noticed that most part of the curve is not observable since angles of refraction larger than about 35° are impossible to get in this material. However, fortunately, the peak of the type II PM contribution can be reached.

The measurements are represented in Fig. 8 together with the simulation results. The experiment could not be continued beyond an angle of incidence of 46° because the light beam was blocked by the sample holder. Anyway, a peak is sufficiently well defined, with its maximum at about 40°. A fairly good agreement is found with the theory, thus confirming that the signal is due to type II PM.

It is also worth mentioning that another peak (not shown in Fig. 8) was observed at negative angles of incidence, in accordance with Fig. 7. This second peak, however, was not perfectly symmetric but had smaller magnitude and was less defined. This discrepancy was attributed to an asymmetry in the angular positions for light blocking at negative and positive angles and/or to low sample quality.

In summary, we have studied the conditions for observing type II phase-matched SHG in FLC's. It has been found that the phenomenon is not usual for conventional materials under common alignments. However, we have presented an example in which the effect has been demonstrated. The angular PM profile is in rather good accordance with the simulations.

ACKNOWLEDGMENTS

One of us (N.P.) thanks the Spanish CICYT for a grant. This work was supported by the Universidad del País Vasco (Project No. 063.310-EB228/95), and CICYT (Project No. MAT94-0717-C02).

[1] D. M. Walba, M. B. Ros, N. A. Clark, R. Shao, K. M. Johnson, M. G. Robinson, J. Y. Liu, and D. J. Doroski, Mol. Cryst. Liq. Cryst. **198**, 51 (1991).

[2] D. M. Walba, M. B. Ros, T. Sierra, J. A. Rego, N. A. Clark, R. Shao, M. D. Wand, R. T. Vohra, K. E. Arnett, and S. P. Velsco, Ferroelectrics **121**, 247 (1991).

[3] K. Schmitt, R. P. Herr, M. Schadt, J. Fünfschilling, R. Buchecker, X. H. Chen, and C. Benecke, Liq. Cryst. **14**, 1735 (1993).

[4] P. Espinet, J. Etxebarria, C. L. Folcia, J. Ortega, M. B. Ros, and J. L. Serrano, Adv. Mater. **8**, 745 (1996).

[5] Y. R. Shen, in *The Principles of Nonlinear Optics* (John Wiley & Sons, New York, 1984), Chap. 6, p. 76.

[6] M. I. Barnik, L. M. Blinov, and N. M. Shtykov, Zh. Eksp. Teor. Fiz. **86**, 1681 (1984) [Sov. Phys. JETP **59**, 980 (1984)].

[7] A. Taguchi, Y. Ouchi, H. Takezoe, and A. Fukuda, Jpn. J. Appl. Phys., Part 2 **28**, L997 (1989).

[8] A. Yariv and P. Yeh, in *Optical Waves in Crystals* (John Wiley & Sons, New York, 1984), Chap. 12, p. 520.

[9] J. Zyss and D. S. Chemla, in *Nonlinear Optical Properties of Organic Molecules and Crystals*, edited by D. S. Chemla and J. Zyss (Academic Press, Orlando, 1987), Chap. II-1, p. 42.

[10] J. Y. Liu, M. G. Robinson, K. M. Johnson, D. M. Walba, M. B. Ros, N. A. Clark, R. Shao, and D. Doroski, J. Appl. Phys. **70**, 3426 (1991).

[11] J. Ortega, C. L. Folcia, J. Etxebarria, M. B. Ros, and J. A. Miguel, Liq. Cryst. **23**, 285 (1997).

[12] J. S. Patel, T. M. Leslie, and J. W. Goodby, Ferroelectrics **59**, 137 (1984).

[13] N. Pereda, C. L. Folcia, J. Etxebarria, J. Ortega, and M. B. Ros, Liq. Cryst. **24**, 451 (1998).